A Pictorial View of Viscosity in Ionic Liquids and the Link to Nanostructural Heterogeneity

Weththasinghage D. Amith,† Juan C. Araque,‡ and Claudio J. Margulis*,†

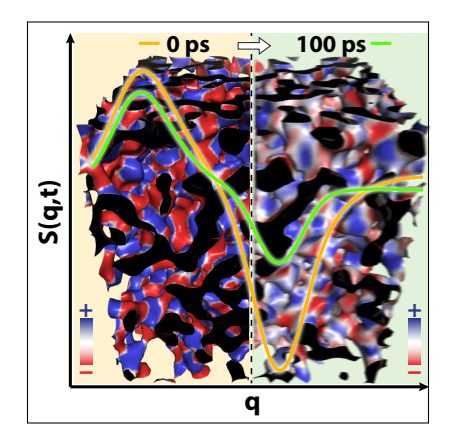
†Department of Chemistry, University of Iowa, Iowa City, Iowa 52242, United States ‡School of Engineering, Benedictine College, Atchison, Kansas 66002, United States

E-mail: claudio-margulis@uiowa.edu

Abstract

Prototypical ionic liquids (ILs) are characterized by three structural motifs associated with (1) vicinal interactions, (2) the formation of positive-negative charge alternating chains or networks and (3) the alternation of these networks with apolar domains. In recent articles, we highlighted that friction and mobility in these systems are nowhere close to being spatially homogeneous. This results in what one could call mechanical heterogeneity where charge networks are intrinsically stiff and charge depleted regions are softer, flexible and mobile. This letter attempts to provide a clear and visual connection between friction—associated with the dynamics of the structural motifs (in particular the charge network)—and recent theoretical work by Yamaguchi linking the time-dependent viscosity of ILs to the decay of the charge alternation peak in the dynamic structure function. We propose that charge-blurring associated with the loss of memory of where positive and negative charges are within networks is the key mechanism associated with viscosity in ILs. An IL will have low viscosity if a characteristic charge blurring decorrelation time t_{charge} is low. With this in mind, engineering new low viscosity ILs reduces to understanding how to minimize this quantity.

Graphical TOC Entry



In a recent set of articles 1-6 we studied in detail the rotational and translational diffusion of solutes dissolved in different ILs as well as the mobility of constituent ions and their internal polar and apolar subcomponents. In all cases the results were conclusive; the charge network (which is the hallmark of all ionic liquids) is stiff and motion of solutes in its proximity is hindered; these are regions of high charge density, high number density and high electrostriction. Even the mobility of small neutral solutes is arrested in these regions; instead, charge depleted regions are mobile and so is diffusion in them. Commonly, each of the three structural motifs in ILs has its own characteristic peak in the structure function (S(q)), $^{1,7-19}$ and more generally in the time dependent dynamic structure function (S(q,t)) which can be obtained either from computer simulations or from inelastic neutron scattering experiments. ^{20–23} For $T \approx 377.4$ K, Fig. 1 shows the computationally derived S(q,t) at four different times for the case of the prototypical IL, 1-Methyl-3-octylimidazolium Bis(trifluoromethylsulfonyl)amide $(Im_{1.8}^+/NTf_2^-)$; the figure also highlights the structural origin or each peak. Around the same time we published our work on the dynamics of ILs, $^{1-6}$ and based on the analysis of S(q,t), Yamaguchi^{24–26} arrived at the conclusion that viscosity in ILs is linked to what Fig. 1 defines as $S(q_{charge}, t)$. In his work, the decay with time of $S(q_{charge}, t)^2$ is equated with that of the stress-tensor Green-Kubo correlation function from which viscosity is computed. In other words, based on this theory, the charge network dynamics and the decay of the stress tensor correlation function are basically one and the same process! It is worth briefly revisiting Yamaguchi's ^{24–26} hypotheses to see how his conclusions are arrived at and how these relate to our findings and that of others on mechanical heterogeneity. 1-6,27 The final goal is to derive a pictorial atomistic view of the physical process responsible for the viscosity in ILs. For this we start with the Green-Kubo expression²⁸ in Eqns. 1,

$$\mu = \int_0^\infty \mu(t)dt = \frac{1}{k_B T V} \int_0^\infty \langle \sigma^{zx}(0)\sigma^{zx}(t)\rangle dt \tag{1}$$

where μ is the bulk viscosity, $\langle \sigma^{zx}(0)\sigma^{zx}(t)\rangle$ is the correlation function of the stress tensor

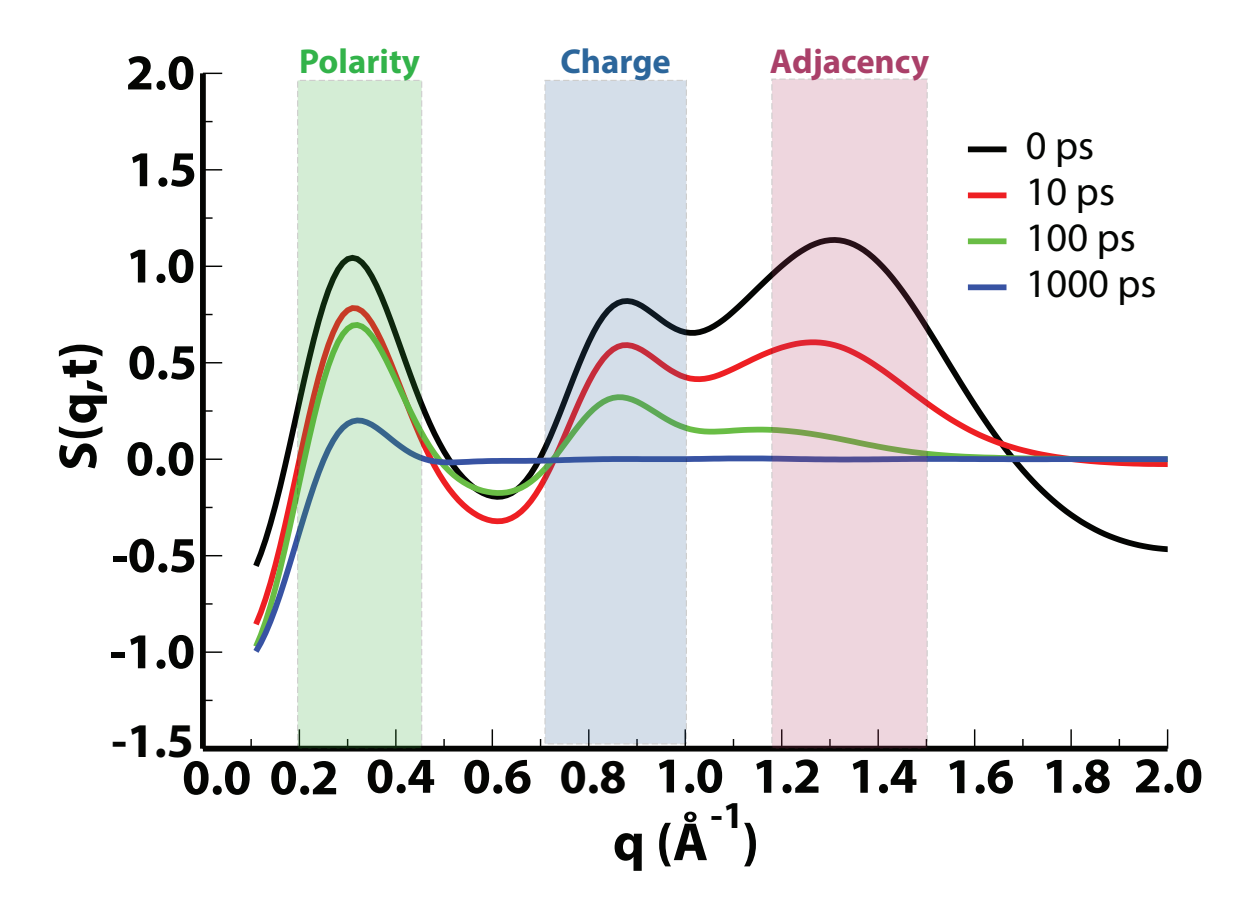


Figure 1: S(q,t) for $\text{Im}_{1,8}^+/\text{NTf}_2^-$ at 0 ps, 10 ps, 100 ps and 1000 ps. The figure highlights the three structural motifs in prototypical ILs, each characterized by a peak in S(q,t=0) that relaxes on its own time scale. Phenomena at lower q (longer distances) decay the slowest. Specifically, the polar-apolar alternation peak $(S(q_{polarity},t))$ –often referred to as a prepeak or a first sharp diffraction peak—decays the slowest and vicinal correlations associated with the adjacency peak $(S(q_{adjacency},t))$ the fastest. The positive-negative charge alternation peak $(S(q_{charge},t))$ associated with the dynamics within the charge network decorrelates on an intermediate time scale. The main argument by Yamaguchi^{24–26} is that it is this intermediate time scale that is the most relevant to viscosity. The separation of these time scales is significant, but the different processes are not completely decorrelated.

and $\mu(t)$ is related to the time dependent liquid structure via the mode coupling theory expression

$$\mu_{MC}(t) = \int \mu_{MC}(q, t) dq \propto \int dq \ q^4 \left[\frac{S'(q)}{S(q)} \right]^2 \left[\frac{S(q, t)}{S(q)} \right]^2. \tag{2}$$

Similar expressions to that on the right hand side of Eqn. 2 appear in multiple previous articles $^{24-26,29-34}$ as well as in the book by Balucani and Zoppi (Eq. 6.110). 28 Yamaguchi's strong hypothesis is that in reality, for ionic liquids, there is only a single q region that significantly contributes to $\mu(t)$. This q region is what in this letter we refer to as q_{charge} ; relaxation of the other liquid features are either too slow or too fast to be relevant. In other words, all q related functions on the right hand side of Eqn. 2 are evaluated at q_{charge} and no integration over q is performed which results in

$$\int \langle \sigma^{zx}(0)\sigma^{zx}(t)\rangle dt \propto \mu \approx \mu_{MC} \propto \int S(q_{charge}, t)^2 dt, \text{ or, } \langle \sigma^{zx}(0)\sigma^{zx}(t)\rangle \propto S(q_{charge}, t)^2.$$
 (3)

In this letter, we treat the mode coupling theory expressions and Yamaguchi's hypothesis as completely empirical and test their validity from a molecular dynamics perspective. In fact, we propose to push his approximation even further by claiming that one should not be looking at the dynamics of $S(q_{charge}, t)$ but instead at that of what in prior work 1,7,8,10,11,13 we have referred to as the cationic head-anionic partial subcomponent of this function $(S^{H-A}(q_{charge}, t))$. In the static case, $S^{H-A}(q)$ carries all the relevant information on structural correlations between charged subcomponents of the liquid. For example, at q_{charge} , this function always shows as what in prior publications we called an antipeak. 1,8,11 This is because $2\pi/q_{charge}$ defines the typical distance between same-charge species in the charge network and there is a significant depletion of probability of finding opposite-charge species at this distance (or this q value); this is clearly depicted at $q \approx 0.85$ Å⁻¹ in Fig. 2. In contrast to the antipeak at q_{charge} , at $q_{polarity}$ ($q \approx 0.3$ Å⁻¹) this function always appears as a peak because $2\pi/q_{polarity}$ is the characteristic distance between charge-networks (independent of charge sign) separated by apolar domains. 13

Since the charge networks are the stiff (highly frictional) liquid regions, it is reasonable to conjecture that $\mu(t)$ should track their dynamics characterized by the time integral of $S^{H-A}(q_{charge},t)^2$. From Fig. 2, we see that the relaxation with respect to time of $S^{H-A}(q,t)$ is significantly faster at q_{charge} than at $q_{polarity}$; this is because one process is associated with shorter-range motion, whereas the other with larger-scale across-networks changes.

Figure 3 shows the integral of the Green-Kubo correlation function of the stress tensor as compared to that of $S^{H-A}(q,t)^2$ for $q_{adjacency}$, q_{charge} and $q_{polarity}$; all functions are normalized to go to one at long time. It is clear from this figure that only the normalized integral of $S^{H-A}(q_{charge},t)^2$ matches the behavior of $\mu(t)/\mu(\infty)$, and whereas this letter shows this only for $\mathrm{Im}_{1,8}^+/\mathrm{NTf}_2^-$, we have preliminary results indicating that the result may be quite generic (data not shown). At this point, the question to answer is what physically happens to the charge network on the time scale t_{charge} associated with the dissipation of correlations in $S^{H-A}(q_{charge},t)^2$? This is the same characteristic time scale for the decay of the stress tensor correlation function beyond which its time integral provides no significant contribution to μ . For example, do charge networks locally vanish? One thing is clear, systems for which this decorrelation time is short tend to have low viscosity and, needless to mention, this is a highly desirable quality for an IL. Understanding the mechanistic aspects of this decorrelation process is of paramount significance to the design of high and low viscosity ILs.

Table S.1 (and corresponding Figs. S.1, S.2, and S.3) provide characteristic times for the decay of $S^{H-A}(q,t)^2$ at $q_{adjacency}$, q_{charge} and $q_{polarity}$ assuming that these functions follow single or double exponential behavior; both procedures result in reasonable fits. Beyond an initial fast relaxation, the more accurate double exponential functions have characteristic decay times of 19.455 ps, 75.758 ps and 416.67 ps at $q = q_{adjacency}$, q_{charge} and $q_{polarity}$ respectively. For 10 ps, 100 ps and 1000 ps which roughly represent $t_{adjacency}$, t_{charge} and $t_{polarity}$, Fig. 4 provides the qualitative pictorial representation we are seeking. Figure 4a shows a portion of the charge network at 0 ps in the form of a color-coded isosurface enclosing the polar portion of the ions. The colors emphasize the typical pattern of charge alternation

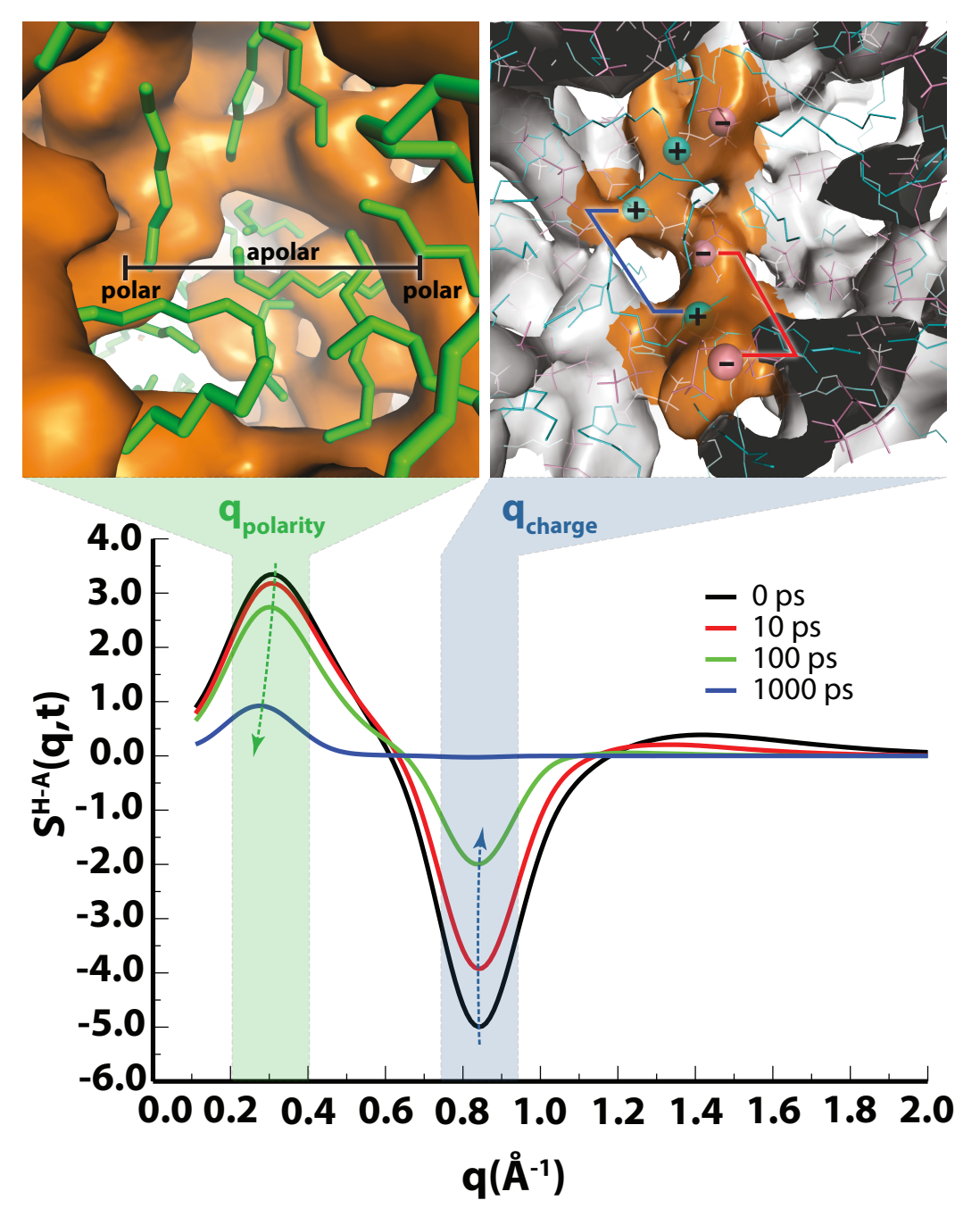


Figure 2: $S^{H-A}(q,t)$ for $\text{Im}_{1,8}^+/\text{NTf}_2^-$ at 0 ps, 10 ps, 100 ps and 1000 ps. The figure highlights the distinct behavior of the cation head-anion subcomponent of S(q,t) within charge networks (antipeak at $q \approx 0.85 \text{ Å}^{-1}$) as opposed to across charge networks (peak at $q \approx 0.3 \text{ Å}^{-1}$). The decay of correlations within charge networks is faster; we propose that the dynamics of the integral of the square of this function evaluated at q_{charge} should track the behavior of $\mu(t)$ (see Fig. 3). Visualizations connected to the antipeak at $q \approx 0.85 \text{ Å}^{-1}$ and the peak at $q \approx 0.3 \text{ Å}^{-1}$ highlight the liquid structural patterns (positive-negative charge alternation vs. polar-apolar alternation) responsible for them. For convenience the cationic head in the visualizations is defined up to the first CH_n groups attached to imidazolium. The actual head definition is up to the second group for the calculation of $S^{H-A}(q,t)$; this is because the force field charges add to +1 up to that group.

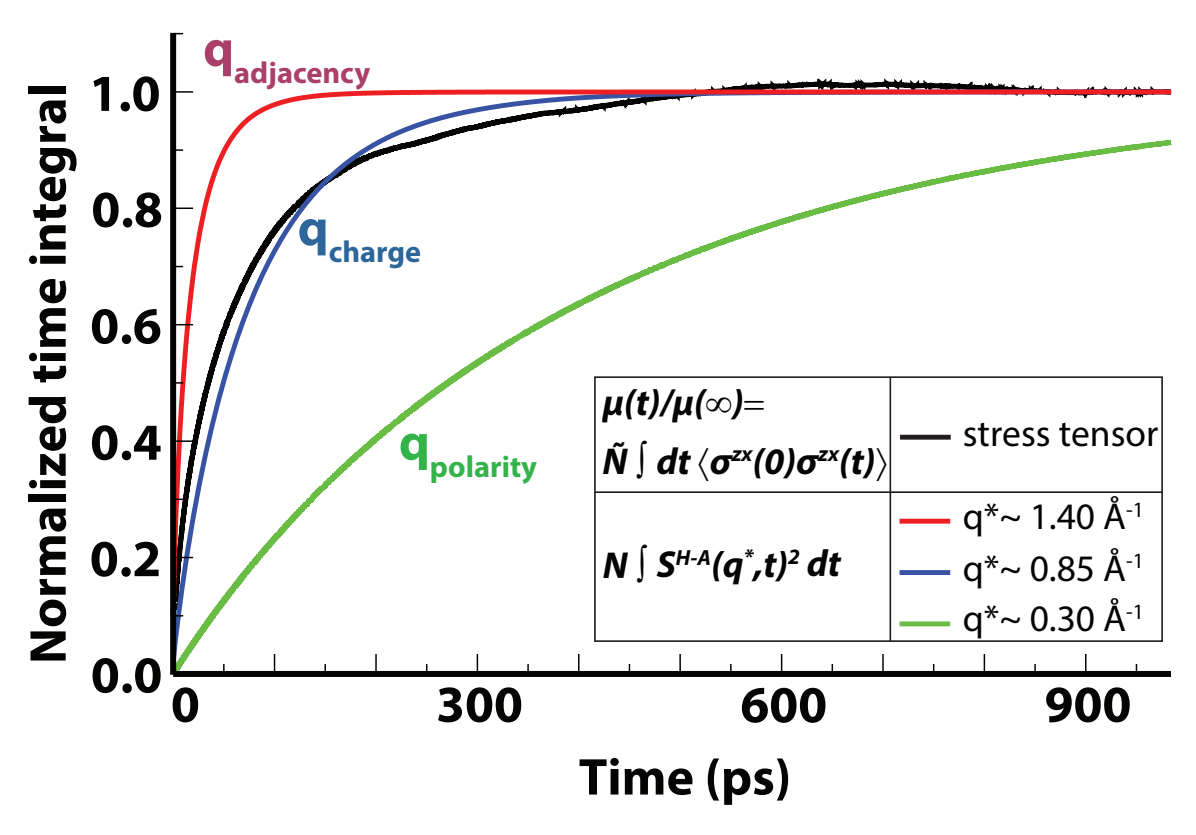


Figure 3: For $\text{Im}_{1,8}^+/\text{NTf}_2^-$ a comparison between the normalized time integral of the Green-Kubo stress tensor autocorrelation function (black line) from which μ is obtained, and that of $S^{H-A}(q,t)^2$ evaluated at $q_{adjacency},\ q_{charge}$ and $q_{polarity}$. The behavior of the normalized time integral of $S^{H-A}(q_{charge},t)^2$ almost perfectly matches that of $\mu(t)/\mu(\infty)$. The long-time cutoff used to normalize $\mu(t)$ was selected based on the prescription by Maginn and coworkers, 35 $N = \left(\int_0^\infty S^{H-A}(q^*,t)^2 dt\right)^{-1},\ \tilde{N} = \left(\int_0^\infty \langle \sigma^{zx}(0)\sigma^{zx}(t)\rangle dt\right)^{-1}$; see the SI for further details on how the infinite time limit is defined for $S^{H-A}(q^*,t)^2$.

within the charge network. Using the original (t=0) ps) location of the charge network, Fig. 4b shows an equal-weights linear combination (see the SI for details) of the colors corresponding to t=0 ps and t=10 ps; since at 10 ps atoms in the charge network have not significantly displaced with respect to t=0 ps, the color associated with the linear combination remains almost the same as in Fig. 4a (an inset in Fig. 4b shows as a cyan mesh the actual network at t=10 ps overlayed with the t=0 ps network in orange). Instead, at 100 ps, the same type of linear combination results in significant charge blurring as can be appreciated from the washed out nature of colors in Fig. 4c. As can be seen from the inset in Fig. 4c, this is because of the significant random displacement of the charge network (cyan mesh) with respect to the time zero network. Whereas the network has not disappeared at 100 ps, ions have displaced enough in random directions that at the location of the original charge network it becomes harder to predict where blue or red patches should be based on where they were at time zero. This is the loss of memory effect that we refer to as charge blurring.

Figure 4d shows a similar representation, but instead treats all charges as belonging to the same "polar" type (enclosed by the orange isosurface). Since after 1000 ps the original polar network has displaced significantly and undergone ionic swaps with other network branches, at the location of the original charge network it becomes harder to predict where polar or apolar patches should be based on where these were at time zero; in other words, this is the time scale for polarity blurring. This is why at the location of the original orange network we find portions that are now orange and portions that are green corresponding to a preponderance of apolar components in the linear combination. Figure 4e shows the t = 0 ps network overlapped with the t = 1000 ps apolar domain represented as a green mesh. It is clear that in random locations the apolar domain has "flooded" what used to be the polar region.

In conclusion, we see that in an IL, the charge network has two main dynamical behaviors. (1) The intra-chain dynamics, what we call in-network *charge blurring*, that is directly

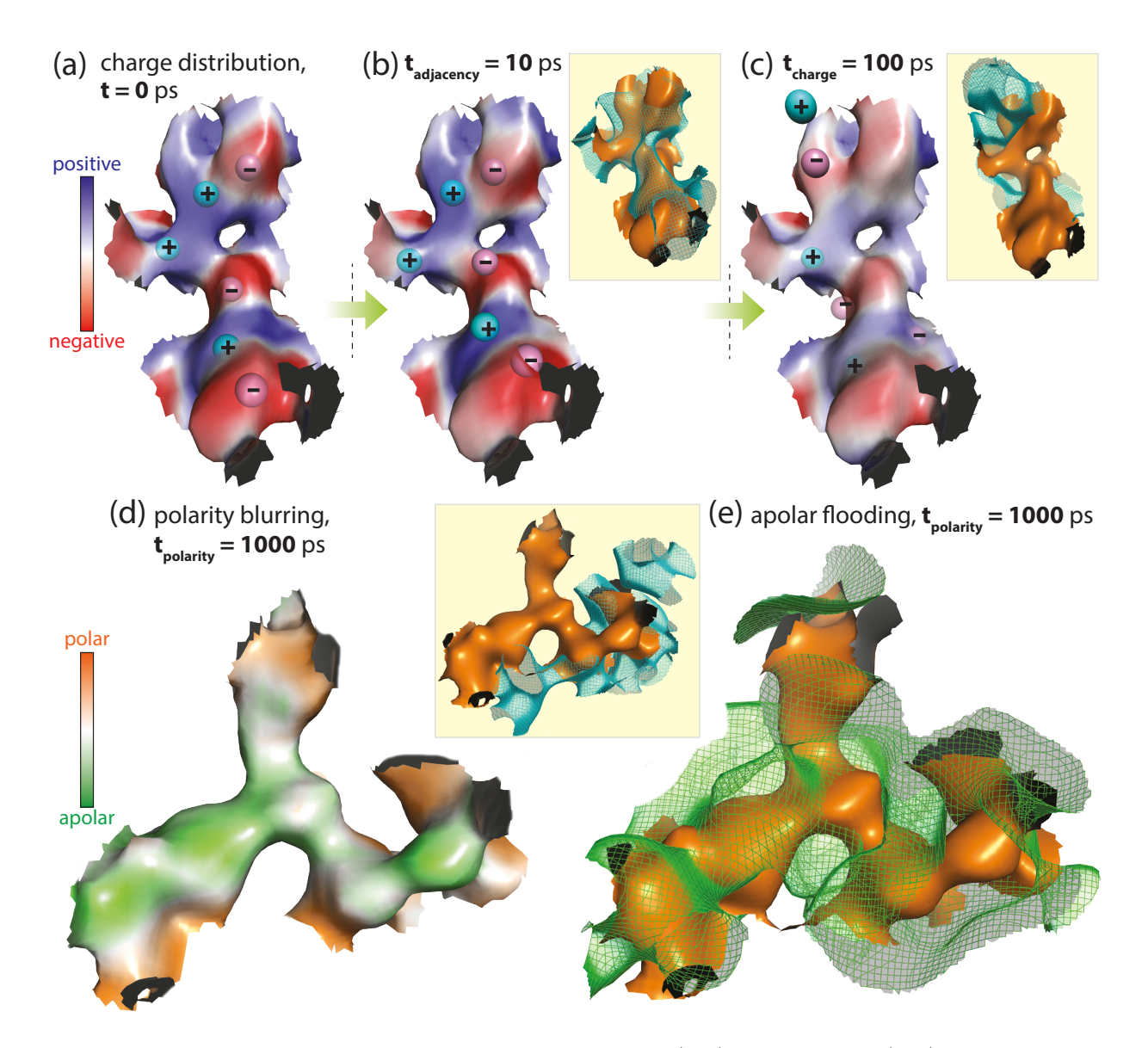


Figure 4: Pictorial view of the time evolution of charge (a-c) and polarity (d-e) at the location of a charge network at time zero. Top row: (a) charge network isosurface at time zero colored according to its initial number density of cationic heads (taken as the imidazolium ring and up to the first CH_n group attached to it) and anions; (b) isosurface colors are the result of a linear combination of the 0 ps and 10 ps colors at the location of the time zero isosurface. Since the colors are almost the same as in (a) there is almost full memory of the original charge ordering; (c) same as (b) but at 100 ps; in this case there is significant charge blurring. In (b-c), the insets show the location of the original charge network (solid orange) and its location (cyan mesh) at 10 ps (b) and 100 ps (c). In (a-c), pink and cyan spheres denote the actual location of the center of mass of anions and cationic-heads, respectively. Bottom row: (d) at 1000 ps, same as b-c except that all charges are considered polar (orange) and cationic apolar tails are green. In (d), the inset shows the location of the original polar network (solid orange) and its actual location at 1000 ps (cyan mesh); (e) at 1000 ps the location of the original polar network depicted by the orange isosurface is partially flooded by apolar cationic tails depicted by the green mesh. See citations 36, 37 and the SI for further details.

linked to viscosity and (2) the across networks dynamics. On the time scale of intra-chain dynamics associated with t_{charge} , positive-negative charge ordering is on its way to becoming decorrelated with that at t=0. In the most simple terms, if we want an IL of low viscosity we need to be able to create a very malleable charge network. Even on the longer $t_{polarity}$ scale, the charge network never really dissipates but instead diffuses and some connections are swapped with those of charge strings nearby. At $t_{polarity}$, where we originally had charge we can now either have tails or charge; put differently, at $t_{polarity}$, the system in on its way to loosing memory of where charges (independent of sign) were at time zero. This process is on a longer time than the decay of the stress tensor correlation function associated with viscosity. Chemical modifications will affect both intra- and across-network processes since their dynamics are not decoupled. Yet, it is only the charge blurring process and not the polarity blurring process that mimics the dynamics of the stress tensor autocorrelation function. We believe that these findings by Yamaguchi and further insight from our group open creative design opportunities to truly target the viscosity behavior of ILs.

Acknowledgement

This work was supported by NSF Grant No. 1664832 awarded to C.J.M. at the University of Iowa; W.D.A and C.J.M. thank the University of Iowa for a generous allocation of high performance computing resources. J.C.A. at Benedictine College gratefully acknowledges the support by the NVIDIA Corporation for the donation of the Quadro P6000 GPU used in generating visualizations for this article.

Supporting Information Available

The Supporting Information is available free of charge at XXX.

Molecular dynamics simulation details, dynamic structure function calculation details, exponential and biexponential time constant fits to the decay of $S^{H-A}(q,t)$ and further details

References

- (1) Araque, J. C.; Hettige, J. J.; Margulis, C. J. Modern Room Temperature Ionic Liquids, a Simple Guide to Understanding Their Structure and How It May Relate to Dynamics. The Journal of Physical Chemistry B 2015, 119, 12727–12740.
- (2) Araque, J. C.; Hettige, J. J.; Margulis, C. J. Ionic liquids—Conventional solvent mixtures, structurally different but dynamically similar. The Journal of Chemical Physics 2015, 143, 134505.
- (3) Araque, J. C.; Yadav, S. K.; Shadeck, M.; Maroncelli, M.; Margulis, C. J. How Is Diffusion of Neutral and Charged Tracers Related to the Structure and Dynamics of a Room-Temperature Ionic Liquid? Large Deviations from Stokes-Einstein Behavior Explained. The Journal of Physical Chemistry B 2015, 119, 7015-7029.
- (4) Araque, J. C.; Daly, R. P.; Margulis, C. J. A link between structure, diffusion and rotations of hydrogen bonding tracers in ionic liquids. *The Journal of Chemical Physics* 2016, 144, 204504.
- (5) Daly, R. P.; Araque, J. C.; Margulis, C. J. Communication: Stiff and soft nano-environments and the "Octopus Effect" are the crux of ionic liquid structural and dynamical heterogeneity. *The Journal of Chemical Physics* **2017**, *147*, 061102.
- (6) Araque, J. C.; Margulis, C. J. In an ionic liquid, high local friction is determined by the proximity to the charge network. *The Journal of Chemical Physics* **2018**, *149*, 144503.
- (7) Kashyap, H. K.; Margulis, C. J. (Keynote) Theoretical Deconstruction of the X-ray Structure Function Exposes Polarity Alternations in Room Temperature Ionic Liquids. ECS Transactions 2013, 50, 301–307.

- (8) Kashyap, H. K.; Hettige, J. J.; Annapureddy, H. V. R.; Margulis, C. J. SAXS antipeaks reveal the length-scales of dual positive–negative and polar–apolar ordering in room-temperature ionic liquids. *Chemical Communications* **2012**, *48*, 5103.
- (9) Kashyap, H. K.; Santos, C. S.; Annapureddy, H. V. R.; Murthy, N. S.; Margulis, C. J.; Castner Jr., E. W. Temperature-dependent structure of ionic liquids: X-ray scattering and simulations. Faraday Discuss. 2012, 154, 133–143.
- (10) Hettige, J. J.; Araque, J. C.; Kashyap, H. K.; Margulis, C. J. Communication: Nanoscale structure of tetradecyltrihexylphosphonium based ionic liquids. *The Journal of Chemical Physics* 2016, 144, 121102.
- (11) Hettige, J. J.; Araque, J. C.; Margulis, C. J. Bicontinuity and Multiple Length Scale Ordering in Triphilic Hydrogen-Bonding Ionic Liquids. The Journal of Physical Chemistry B 2014, 118, 12706–12716.
- (12) Hettige, J. J.; Kashyap, H. K.; Margulis, C. J. Communication: Anomalous temperature dependence of the intermediate range order in phosphonium ionic liquids. *The Journal of Chemical Physics* **2014**, *140*, 111102.
- (13) Hettige, J. J.; Kashyap, H. K.; Annapureddy, H. V. R.; Margulis, C. J. Anions, the Reporters of Structure in Ionic Liquids. *The Journal of Physical Chemistry Letters* **2012**, 4, 105–110.
- (14) Annapureddy, H. V. R.; Kashyap, H. K.; Biase, P. M. D.; Margulis, C. J. What is the Origin of the Prepeak in the X-ray Scattering of Imidazolium-Based Room-Temperature Ionic Liquids? *The Journal of Physical Chemistry B* 2010, 114, 16838–16846.
- (15) Russina, O.; Triolo, A.; Gontrani, L.; Caminiti, R.; Xiao, D.; Jr, L. G. H.; Bartsch, R. A.; Quitevis, E. L.; Pleckhova, N.; Seddon, K. R. Morphology and intermolecular dynamics of 1-alkyl-3-methylimidazolium

- bis{(trifluoromethane)sulfonyl}amide ionic liquids: structural and dynamic evidence of nanoscale segregation. *Journal of Physics: Condensed Matter* **2009**, *21*, 424121.
- (16) Russina, O.; Gontrani, L.; Fazio, B.; Lombardo, D.; Triolo, A.; Caminiti, R. Selected chemical—physical properties and structural heterogeneities in 1-ethyl-3-methylimidazolium alkyl-sulfate room temperature ionic liquids. *Chemical Physics Letters* 2010, 493, 259–262.
- (17) Russina, O.; Triolo, A.; Gontrani, L.; Caminiti, R. Mesoscopic Structural Heterogeneities in Room-Temperature Ionic Liquids. *The Journal of Physical Chemistry Letters* **2011**, *3*, 27–33.
- (18) Hayes, R.; Warr, G. G.; Atkin, R. Structure and Nanostructure in Ionic Liquids. *Chemical Reviews* **2015**, *115*, 6357–6426.
- (19) Greaves, T. L.; Drummond, C. J. Protic Ionic Liquids: Evolving Structure–Property Relationships and Expanding Applications. *Chemical Reviews* **2015**, *115*, 11379–11448.
- (20) Chathoth, S. M.; Mamontov, E.; Fulvio, P. F.; Wang, X.; Baker, G. A.; Dai, S.; Wesolowski, D. J. An unusual slowdown of fast diffusion in a room temperature ionic liquid confined in mesoporous carbon. EPL (Europhysics Letters) 2013, 102, 16004.
- (21) Kofu, M.; Nagao, M.; Ueki, T.; Kitazawa, Y.; Nakamura, Y.; Sawamura, S.; Watanabe, M.; Yamamuro, O. Heterogeneous Slow Dynamics of Imidazolium-Based Ionic Liquids Studied by Neutron Spin Echo. The Journal of Physical Chemistry B 2013, 117, 2773–2781.
- (22) Yamamuro, O.; Yamada, T.; Kofu, M.; Nakakoshi, M.; Nagao, M. Hierarchical structure and dynamics of an ionic liquid 1-octyl-3-methylimidazolium chloride. *The Journal of Chemical Physics* **2011**, *135*, 054508.

- (23) Russina, O.; Beiner, M.; Pappas, C.; Russina, M.; Arrighi, V.; Unruh, T.; Mullan, C. L.; Hardacre, C.; Triolo, A. Temperature Dependence of the Primary Relaxation in 1-Hexyl-3-methylimidazolium bis{(trifluoromethyl)sulfonyl}imide. *The Journal of Physical Chemistry B* **2009**, *113*, 8469–8474.
- (24) Yamaguchi, T. Mode-coupling theoretical study on the roles of heterogeneous structure in rheology of ionic liquids. *The Journal of Chemical Physics* **2016**, *144*, 124514.
- (25) Yamaguchi, T. Experimental study on the relationship between the frequency-dependent shear viscosity and the intermediate scattering function of representative viscous liquids. *The Journal of Chemical Physics* **2016**, *145*, 194505.
- (26) Yamaguchi, T. Coupling between the mesoscopic dynamics and shear stress of a room-temperature ionic liquid. *Physical Chemistry Chemical Physics* **2018**, *20*, 17809–17817.
- (27) Veldhorst, A. A.; Ribeiro, M. C. C. Mechanical heterogeneity in ionic liquids. *The Journal of Chemical Physics* **2018**, *148*, 193803.
- (28) Balucani, U.; Zoppi, M. *Dynamics of the Liquid State*; Oxford Science Publications, 1994.
- (29) Balucani, U.; Vallauri, R.; Gaskell, T. Stress autocorrelation function in liquid rubidium. *Physical Review A* **1988**, *37*, 3386–3392.
- (30) Geszti, T. Pre-vitrification by viscosity feedback. *Journal of Physics C: Solid State Physics* **1983**, *16*, 5805–5814.
- (31) Yamaguchi, T.; Faraone, A. Analysis of shear viscosity and viscoelastic relaxation of liquid methanol based on molecular dynamics simulation and mode-coupling theory.

 The Journal of Chemical Physics 2017, 146, 244506.
- (32) Yamaguchi, T.; Koda, S. Mode-coupling theoretical analysis of transport and relaxation

- properties of liquid dimethylimidazolium chloride. The Journal of Chemical Physics **2010**, 132, 114502.
- (33) Yamaguchi, T.; Hirata, F. Site—site mode-coupling theory for the shear viscosity of molecular liquids. *The Journal of Chemical Physics* **2001**, *115*, 9340–9345.
- (34) Yamaguchi, T.; Mikawa, K.; Koda, S.; Fujii, K.; Endo, H.; Shibayama, M.; Hamano, H.; Umebayashi, Y. Relationship between mesoscale dynamics and shear relaxation of ionic liquids with long alkyl chain. *The Journal of Chemical Physics* **2012**, *137*, 104511.
- (35) Zhang, Y.; Otani, A.; Maginn, E. J. Reliable Viscosity Calculation from Equilibrium Molecular Dynamics Simulations: A Time Decomposition Method. *Journal of Chemical Theory and Computation* **2015**, *11*, 3537–3546.
- (36) Schultz, A. J.; Hall, C. K.; Genzer, J. Obtaining Concentration Profiles from Computer Simulation Structure Factors. *Macromolecules* **2007**, *40*, 2629–2632.
- (37) Schultz, A. J. Modeling and Computer Simulation of Block Copolymer/Nanoparticle Composites. Ph.D. thesis, North Carolina State University, Raleigh, NC 27695, 2004.